Advanced Lab Course

Experiment

Quantum Hall Effect

Experimenter	David Urbaniak
E-Mail	davidpaul.urbaniak@stud.uni-goettingen.de
Co-Experimenter	Aaron Globisch
E-Mail	a.globisch@stud.uni-goettingen.de
Date of the experiment	27.09.2023
Tutor	Dr. Jörg Malindretos

Contents

1 Introduction

In the year 1980 von Klitzing et. al measured the quantum Hall effect (QHE) for the first time. During the Hall measurements on a two dimensional electron gas (2DEG) he observed the vanishing of the longitudinal conductivity and plateaus in the transversal resistivity where the longitudinal conductivity vanishes. The values of these Plateaus were 25813 Ω/ν. With ν being an integer. The fascinating characteristic of this value is that it can be expressed with h/e^2. The plateaus in resistivity are therefore linked to the fundamental constants. Apart from the so called integer QHE, a second type exists. In the fractional QHE the plateaus in resistivity appear in values of fractions of e. The understanding of the underlying physics is a current topic of research.
In this lab course the measurements of the classical and the integer quantum Hall effect are investigated.

2 Theory

2.1 Electrical conductivity of semiconductors

The following section briefly describes the electrical conductivity of semiconductors. For a more detailed description see [1, 2].

Semiconductors have a band gap of up to a few electron volt between the so called conduction and valance band. Electrons in the conduction band or holes in the valence band contribute to the charge transport. The charge carrier density n in the conduction band is temperature dependent. This dependence can be categorised in three ranges. The intrinsic-, the saturation - and the freeze-out-range, which can be seen in figure 1. Apart from the electrons in the conduction bands, unoccupied states in the valance band can also contribute to the charge transport. These unoccupied states are called holes and carry a positive charge.

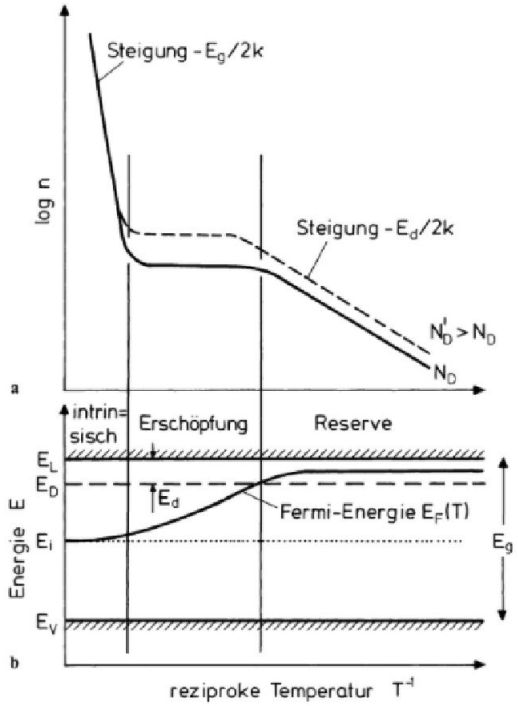

Figure 1: Schematic of the charge carrier density in semiconductors [3].

Apart from the charge carrier density, the charge carrier mobility μ plays an important role for the description of charge transport. The mobility is influenced by scattering events. The charge carriers are mainly scattered by defects and phonons, depending on temperature. This temperature dependence of the mobility μ is depicted in figure 2.

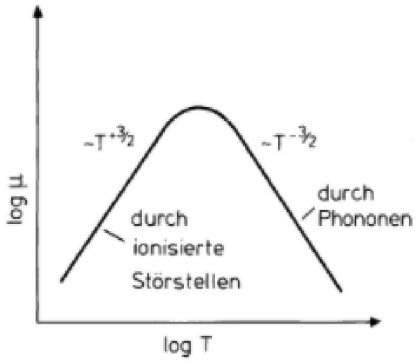

Figure 2: Temperature dependence of the charge carrier mobility [3].

2.2 Van der Pauw Measurement

One is able to determine the specific resistivity and to observe the Hall effect of an arbitrarily shaped sample with the method named after L.J. van der Pauw. However, this method can only be used if the sample is contacted on the edges and if these contacts are small compared to the sample itself. Additional to this requirements the sample has to be uniform, meaning that the sample is of one height and forms an uninterrupted coherent area. Figure 3 shows a schematic of the measurement setup.

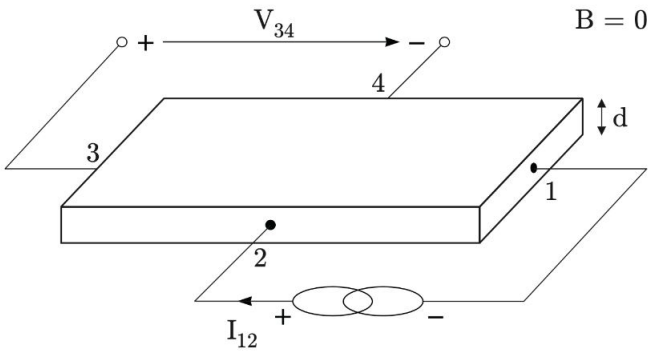

Figure 3: Schematic of the measurement setup for a Van der Pauw measurement [4].

The van der Pauw resistivity R_{ijkl} can be determined with

$$R_{1234} = \frac{V_{34}}{I_{21}} \quad . \tag{1}$$

Where V_{34} is the voltage between contact 3 and 4 and I_{12} is the current flowing between contact 1 and 2.
Because of the arbitrarily shaped sample, a correction factor f has to be introduced. For this, the symmetry factor Q is defined as

$$Q_A = \frac{R_{2134} - R_{1234}}{R_{3241} - R_{2341}} \quad \text{and} \quad Q_B = \frac{R_{4312} - R_{3412}}{R_{1423} - R_{4123}} \quad . \tag{2}$$

The correction factor f is then defined as

$$f \backsimeq 1 - 0.34657A - 0.09236A^2 \quad \text{with} \quad A = \left[\frac{Q-1}{Q+1}\right]^2 \quad . \tag{3}$$

The specific resistance ρ can then be calculated with with

$$\begin{aligned}\rho = \frac{1}{8}\frac{\pi d}{ln2}\left[f_A\left(R_{2134} - R_{1234} + R_{3241} - R_{2341}\right) + \right. \\ \left. f_B\left(R_{4312} - R_{3412} + R_{1423} - R_{4123}\right)\right] \quad .\end{aligned} \tag{4}$$

And the charge carrier mobility μ is with

$$\mu = \frac{|R_H|}{\rho} \quad . \tag{5}$$

Here R_H is the Hall-factor, which is defined as

$$\begin{aligned}R_H = \frac{1}{8}\frac{d}{B_z}\left[(R_{3142}(B+) - R_{1342}(B+) + R_{1342}(B-) - R_{3142}(B-)) + \right. \\ \left. (R_{4213}(B+) - R_{2413}(B+) + R_{2413}(B-) - R_{4213}(B-))\right] \quad .\end{aligned} \tag{6}$$

The direction of the magnetic field is indicated with $B+$ and $B-$, referring to the positive and negative z-direction. The Hall-factor is also needed to calculate the charge carrier concentration

$$n = \frac{1}{e \cdot R_H} \quad . \tag{7}$$

2.3 Classical Hall Effect

The classical Hall effect is one of the fundamental measurements in the investigation of the electrical properties of semiconductors. It is used to determine the charge carrier concentration, mobility and type of majority charge carrier type. As can be seen in figure 4 a rectangular sample with four contacts is needed for the measurement. If a voltage is applied between to contacts, a current will flow. This direction is set to be the x-direction. An applied magnetic field B perpendicular to the charge flow is applied in z-direction. Because of the electric field the Lorentz-force F_L will bend the trajectories of the carriers. This leads to a charge accumulation on one side of the sample, which leads to the buildup of an electric field in y-direction. An equilibrium is reached when the force of the electric field is equal and opposite to the Lorentz-force. The potential difference due to the charge accumulation is measured and called Hall-voltage U_H.

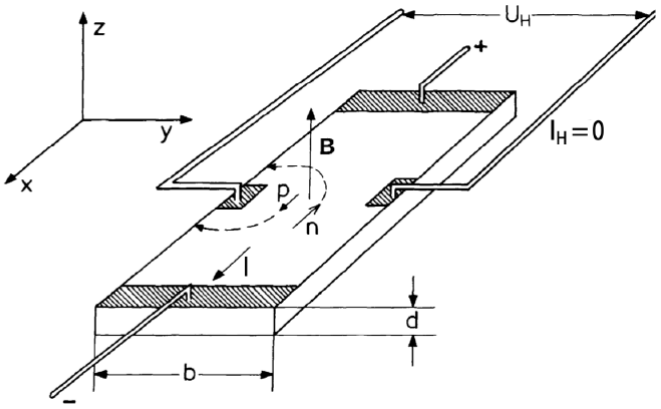

Figure 4: Schematic of a Hall-effect measurement [3].

To calculate the charge carrier mobility and concentration equations (5) and (7) are used. However, it is also possible to express the Hall-factor R_H and thus the charge carrier concentration n as a function of the hall-voltage U_H, current I, thickness of the sample d and magnetic field B_z, when using a Hall-bar structure as a measurement setup.

$$R_H = \frac{U_H \cdot d}{I \cdot B_z} = \frac{1}{n \cdot e} \quad . \tag{8}$$

The charge carrier mobility then can be rewritten as

$$\mu = \frac{I}{V_x \cdot en} \cdot \frac{l_x}{bd} \quad . \tag{9}$$

Here $\sigma = j/E$ with an electric field $E_x = l_x/V_x$ and $j = I/(bd)$ are used because of the sample geometry shown in figure 4. For a more detailed description of the Hall effect see Hunklinger or Gross-Marx [1, 2].

2.4 Quantum Hall Effect

At large magnetic fields, one finds deviations from the classical Hall effect. Plateaus appear in the Hall resistance which are material independent and can be described only using fundamental constants.

$$R_H = \rho_{xy} = \frac{1}{\nu}\frac{h}{e^2} \qquad \text{with} \qquad \nu \in \mathbb{N} \quad . \tag{10}$$

With the Planck-constant h, elementary charge e and the fill factor ν. In addition to the plateaus in the transversal resistance, the longitudinal resistance ρ_{xx} shows so-called Shubnikov-de Haas oscillations.

To understand these oscillations one needs to look at the charge transport in the sample. Due to the confining potential at the edges of the sample the Landau level are bend upwards, as can be seen in figure 5a. If the Fermi energy now lies in-between two Landau level, it will cross the Landau level at the edges. This leads to the formation of conducting edge channels. As displayed in figure 5b the charge carriers get reflected at the edges of the sample. However, back-scattering is suppressed due to the applied magnetic field. This leads to a scipping-like transport. The charge carriers flow in different directions on the opposite side of the sample due to the Lorentz force. The charge transport inside of these channels is quasi-ballistic, which is why the longitudinal resistance vanishes. If the Fermi energy now lies within a Landau level back-scattering between the edge channels becomes possible and there is a peak in the longitudinal resistance. Therefore if one sweeps the Fermi-energy or the magnetic field the mentioned oscillations occur.

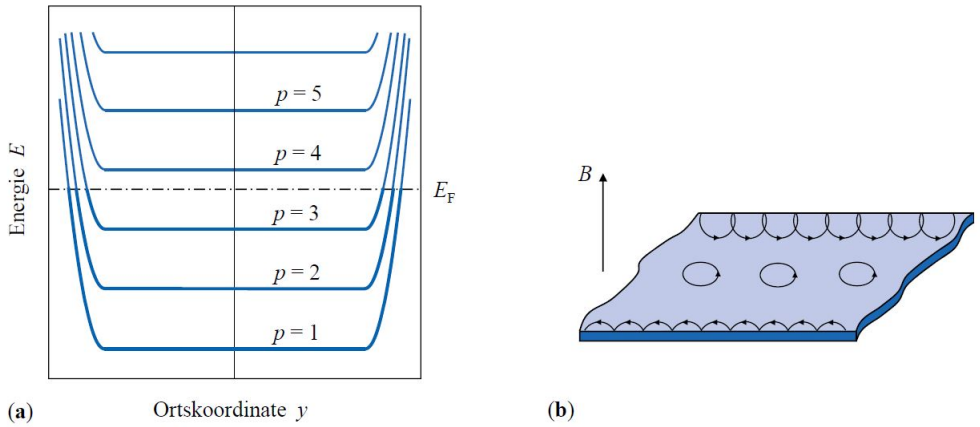

Figure 5: Edge states of a two dimensional electrongas in a finte smaple. a) Landau level bending at the edges of the sample. b) Scipping orbits at the edges of the sample. [2]

Solving the Schrödinger equation for such a system leads to the expression

$$n_{2D} = \eta \frac{eB}{h} \tag{11}$$

for the charge carrier density inside of a Landau level. For a more detailed description see [1] chapter 10.5. In this case η represents the spin degeneracy and thus yields $\eta = 2$.

To determine the sheet carrier concentration one looks at two consecutive minima of the Shubnikov-de Haas oscillations.

$$n_{2D} = \frac{2e}{h}\left(\frac{1}{B_{i+1}} - \frac{1}{B_i}\right)^{-1} = \frac{2e}{h}\left(\Delta\frac{1}{B}\right)^{-1} \quad . \tag{12}$$

3 Experimental Methode

First, the van der Pauw measurement was performed at room temperature. An AlGaN/GaN heterostructure was measured at magnetic field strengths of 300, 400, 500 and 600 mT. The sample was carefully placed inside of the magnet, so that it was perpendicular to the magnetic field.

Next, a Hall-bar structure which consists of an InGaAs/InP heterostructure was used for the Hall effect measurement. Again the sample was carefully positioned inside the magnet in such a way that it was perpendicular to the magnetic field. After ensuring that all contacts work at room temperature, the cryostat was cooled down to 6 K using liquid helium. Now measurements of the Hall resistance and the longitudinal voltage were taken at temperatures reaching from 6 K back to room temperature. For the Hall resistance, the magnetic field was varied between 200 and 500 mT in steps of 50 mT. For the voltage measurement the current was varied between -0.1 and 0.1 mA in steps of 0.05 mA.

The measurement of the Quantum Hall effect was not performed. Here a data set was provided.

4 Results

This section shows and discusses the results of the experiments conducted as stated in section 3.

4.1 Van der Pauw Measurement

From the data the resistanceses R_{ijkl} were extracted as described in chapter 2.2. The determined correction factors f_A and f_B are

$$\begin{aligned} f_A &= 0.9921 \\ f_B &= 0.9913 \quad . \end{aligned}$$

With these correction factors the specific resistance ρ can be calculated with formula (4) and the Hall-factor with equation (6), where in both of these formulas the thickness d of

the sample is the unit width of the 2DEG. With these values the charge carrier density n for the different magnetic fields can be determined with equation (7)

$$\begin{aligned} n_{300\mathrm{mT}} &= 2.46 \cdot 10^{17}\ \mathrm{m}^{-2} \\ n_{400\mathrm{mT}} &= 2.44 \cdot 10^{17}\ \mathrm{m}^{-2} \\ n_{500\mathrm{mT}} &= 2.43 \cdot 10^{17}\ \mathrm{m}^{-2} \\ n_{600\mathrm{mT}} &= 2.42 \cdot 10^{17}\ \mathrm{m}^{-2} \quad . \end{aligned}$$

And the corresponding charge carrier mobilities μ with equation (5)

$$\begin{aligned} \mu_{300\mathrm{mT}} &= 3.91 \cdot 10^{-2}\ \mathrm{m}^2\mathrm{V}^{-1}\mathrm{s}^{-1} \\ \mu_{400\mathrm{mT}} &= 3.93 \cdot 10^{-2}\ \mathrm{m}^2\mathrm{V}^{-1}\mathrm{s}^{-1} \\ \mu_{500\mathrm{mT}} &= 3.95 \cdot 10^{-2}\ \mathrm{m}^2\mathrm{V}^{-1}\mathrm{s}^{-1} \\ \mu_{600\mathrm{mT}} &= 3.96 \cdot 10^{-2}\ \mathrm{m}^2\mathrm{V}^{-1}\mathrm{s}^{-1} \quad . \end{aligned}$$

Averaging over these values leads to a charge carrier density $n = (2.44 \pm 0.02) \cdot 10^{17}\ \mathrm{m}^{-2}$ and a mobility $\mu = (3.94 \pm 0.02) \cdot 10^{-2}\ \mathrm{m}^2\mathrm{V}^{-1}\mathrm{s}^{-1}$. The error is the standard deviation.

Figure 6 displays the the Hall-voltage as a function of the applied magnetic field. Due to the sample geometry a difference in the Hall-voltage can be observed in the different directions. Additional, a varying B-field dependence depending on the polarity of the B-field as well as the applied current can be observed.

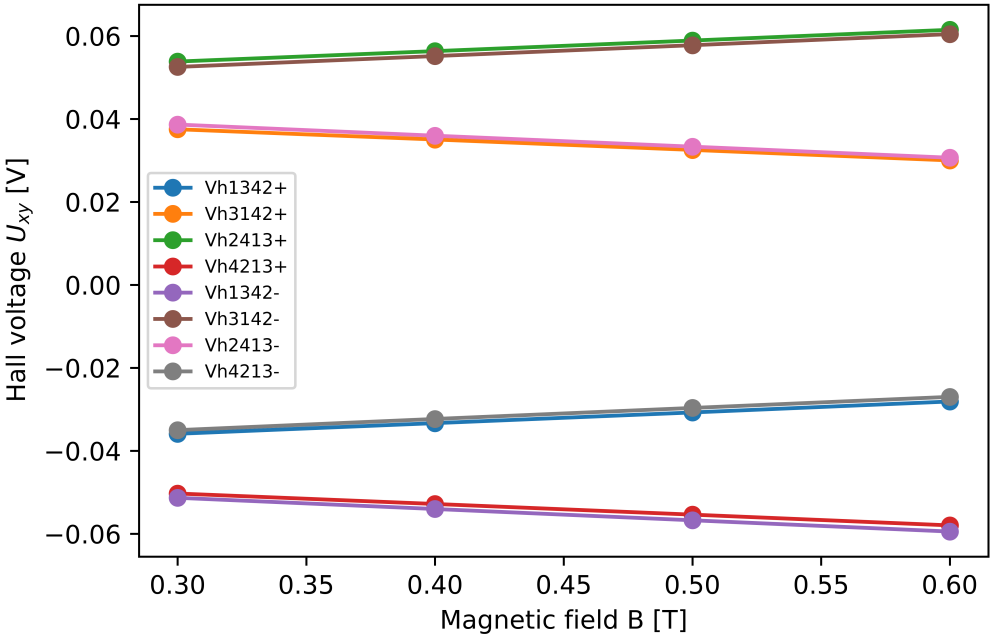

Figure 6: Hall voltage U_{xy} as a function of magnetic field B in the Van der Pauw measurement. The direction of the magnetic field is labelled with + and -.

At zero magnetic field the Hall resistance should go through zero. However an offset is visible. This nicely depicts why it is necessary to average over all combinations of the contacts when using the Van der Pauw method.

4.2 Classical Hall Effect

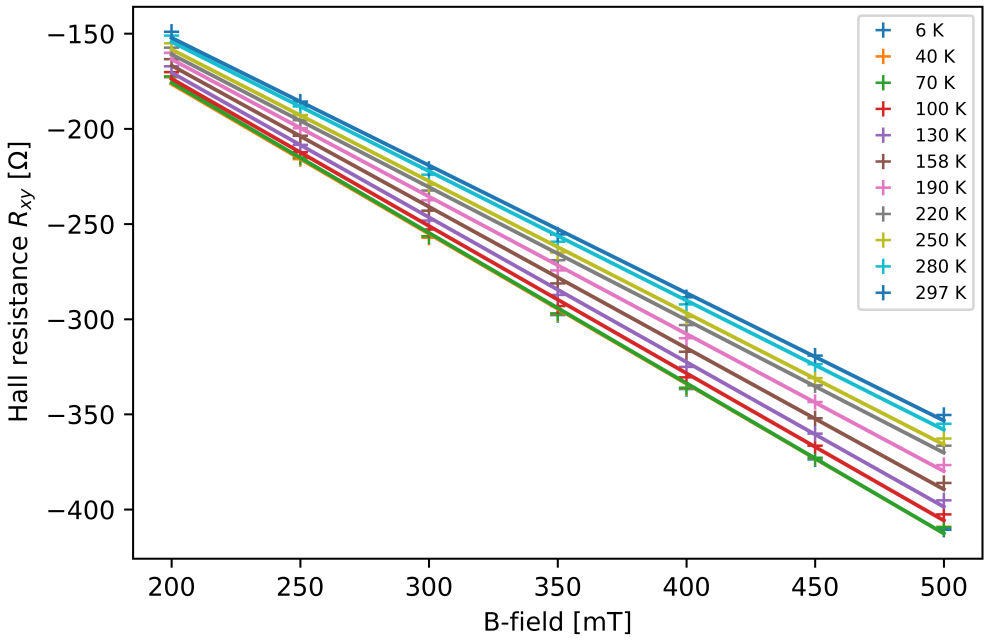

Figure 7: Hall resistance R_{xy} in Ω as a function of magnetic field B in mT for different temperatures. Displayed are the measured values marked with + and a linear regression.

Figure 7 displays the Hall resistance R_{xy} as a function of the magnetic field B for different temperatures. The measured data points are marked with +. The linear regression shows a systematic deviation from the data points. At all temperatures, the data points at the lowest and highest magnetic field are above the regression curve, while at medium field strengths the regression is above the data point. A stochastic error is unlikely because this behaviour is observed at every temperature. An explanation for this could be an error in the calibration of the electromagnet, which leads to a small deviation between the applied current through the magnet and the resulting magnetic field. Figure 8 shows the longitudinal voltage U_{xx} as a function of the applied current I. It can be seen, that the point at which no voltage is measured is not at zero current. This is an additional argument for an error in the calibration.

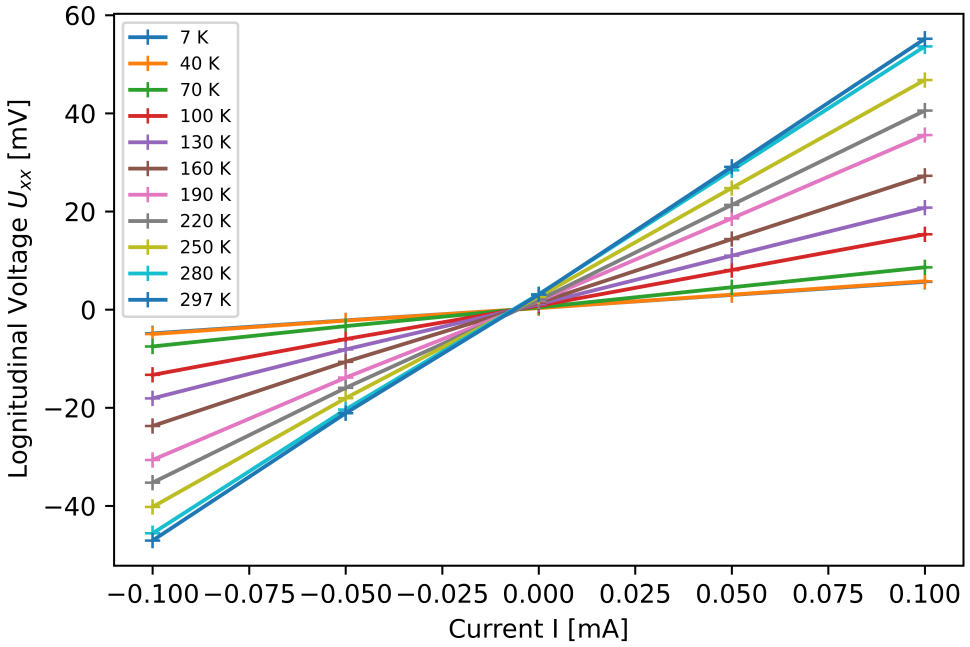

Figure 8: Longitudinal Voltage U_{xx} in mV as a function of the applied current I in mA for different temperatures during the hall measurement.

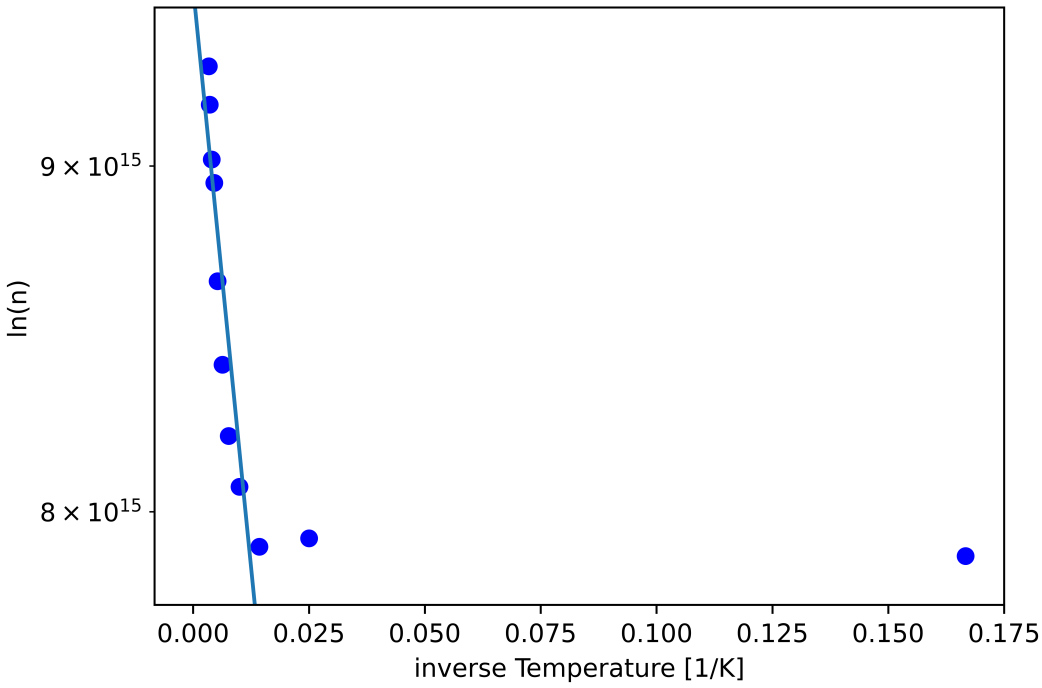

Figure 9: Arrheniusplot of the charge carrier density n as a function of the inverse temperature. Additionally the fit function to extract the activation energy is displayed.

To extract the activation energy the charge carrier density n as a function of the inverse temperature is displayed in figure 9. With a fit of $n = a \cdot exp(-E_A/2k_BT)$ the activation energy E_A can be extracted. Here a is a constant, k_B is the Boltzmann constant and T is the temperature. This results in an activation energy of $E_A = 5.7 \pm 0.9$ meV. Because the activation energy is three orders of magnitude smaller than the bandgap, thermal activation of charge carriers can not explain the behaviour in figure 9. However, the increase in charge carrier density can be explained by trap states that are close to the conduction band.

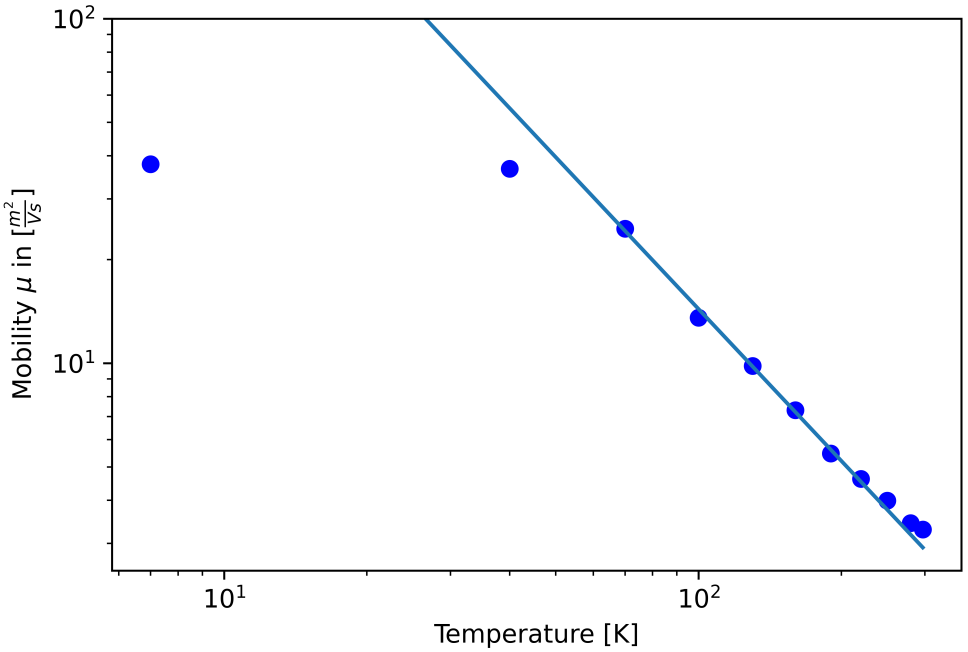

Figure 10: Double logarithmic plot of the charge carrier mobility μ as a function of the temperature T.

Figure 10 displays a double logarithmic plot of the charge carrier mobility μ as a function of the temperature T. For higher temperatures (T $\geq$ 90 K) one can extract the temperature exponent with

$$\mu(T) = a \cdot T^b + c \quad .$$

With the fit parameters a, b and c. The fit results in an exponent of $b = -1.46 \pm 0.03$, which includes the true value of the coefficient with 99% chance. The exponent indicates the phonon interaction which is described in chapter 2.1.

4.3 Quantum Hall Effect

Figure 11 depicts the Hall-resistance R_{xy} as a function of the magnetic field B at a temperature of 2 K. The plateaus at units of h/e^2 are clearly visible at higher magnetic fields. The values of the plateaus ranging from filling factor from $\nu = 5$ to $\nu = 12$ are plotted in the graph. Uneven plateaus with $\nu > 7$ can not be observed in the data, which correlates to the spin-degeneracy in the Landau-levels. Deviations from the expected plateaus can be observed, which increase with increasing magnetic field. These deviations

originate from a conducting channel at the surface of the sample, due to damages caused by an etching process during the sample fabrication.

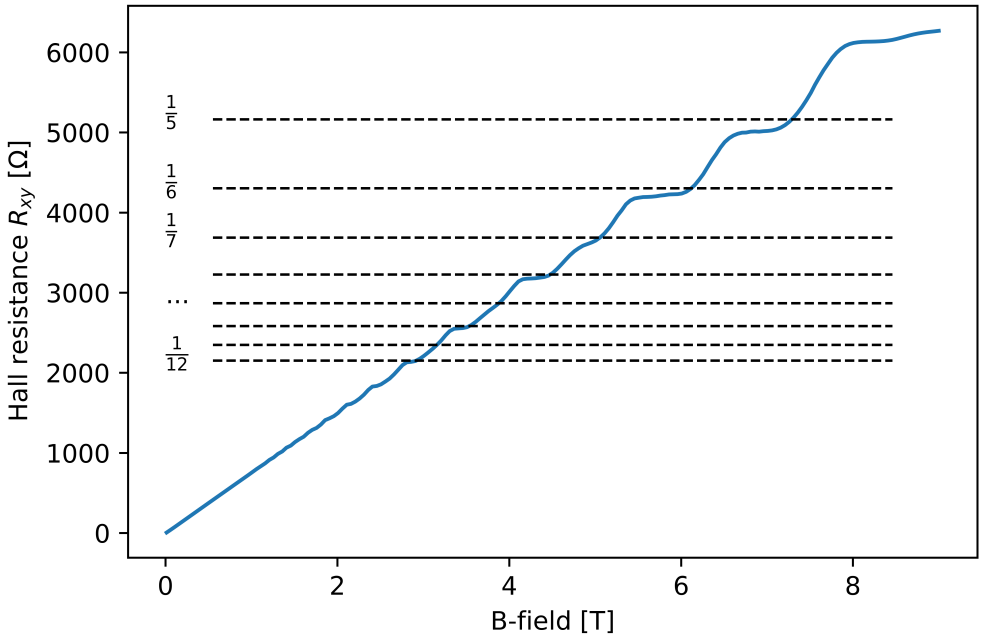

Figure 11: Hall resistance as a function of the magnetic field with the expected plateaus of the quantum hall effect.

In figure 12 the longitudinal resistance is plotted as a function of the reciprocal magnetic field to estimate the charge carrier density as described in chapter 2.4. The constant distances in the Shubnikov-de Haas oscillations of $\Delta\frac{1}{\mathrm{B}} = 0.06\ \mathrm{T}^{-1}$ lead to a charge carrier density of

$$n = 8.05 \cdot 10^{15}\mathrm{m}^{-2} \quad .$$

This is in agreement with the measurements of the classical Hall-effect (see figure 9).
It is to mention that the resistances show an underground, which increases with increasing magnetic field. This resistance originates from the charge conducting channel at the surface of the sample, mentioned before.

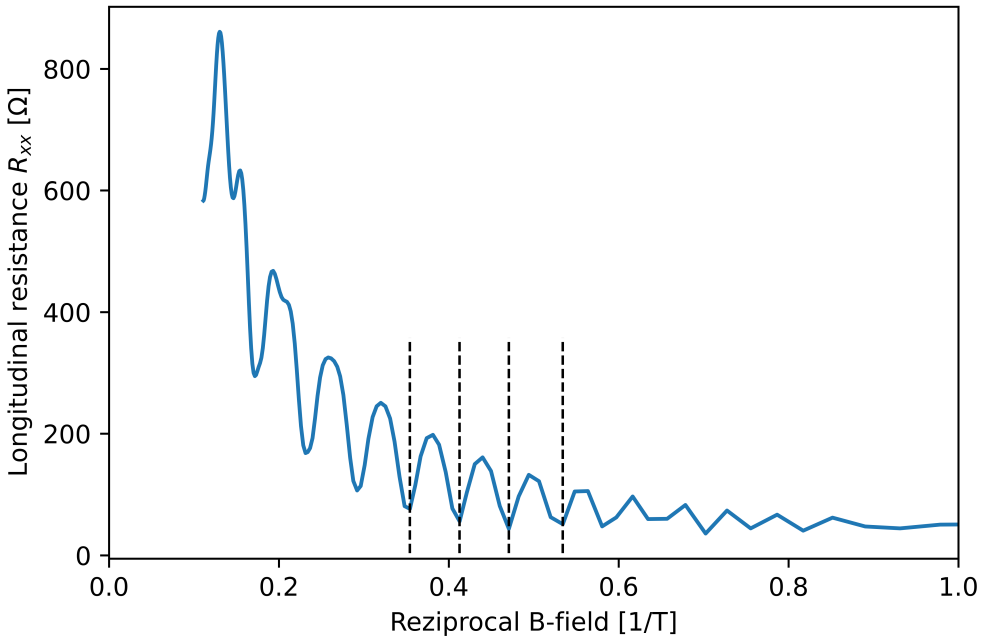

Figure 12: Longitudinal resistance as a function of the reciprocal magnetic field

References

[1] Rudolf Gross and Achim Marx. *Festkörperphysik*. Oldenbourg Wissenschaftsverlag Verlag, 2012.

[2] Siegfried Hunklinger. Festkörperphysik, 2018.

[3] Harald Ibach and Hans Lüth. *Festkörperphysik: Einführung in die Grundlagen*. springer-verlag, 2009.

[4] Joerg Malindretos. Lab course instructions to fm.qhe: quantum-hall-effect.